

## Supporting Information

for the Communication Entitled

### Electroluminescence Based on Thermally Activated Delayed Fluorescence Generated by a Spirobifluorene Donor-Acceptor Structure

Tetsuya Nakagawa<sup>a</sup>, Sung-Yu Ku<sup>b</sup>, Ken-Tsung Wong<sup>b\*</sup> and Chihaya Adachi<sup>a\*</sup>

<sup>a</sup>Center for Organic Photonics and Electronics Research (OPERA), Kyushu University, Motoooka 744,  
Nishi, Fukuoka 819-0395, Japan

<sup>b</sup>Department of Chemistry, National Taiwan University, Taipei 10617, Taiwan

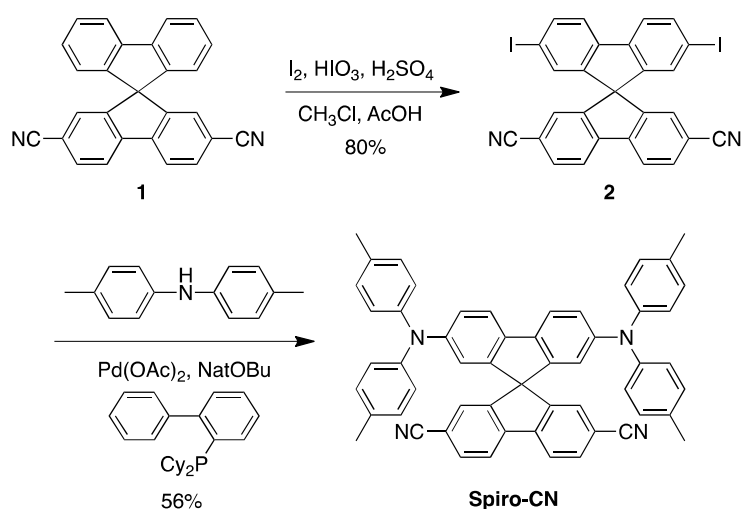
E-mail address: adachi@cstf.kyushu-u.ac.jp; kenwong@ntu.edu.tw

#### Contents

1. Synthesis procedure of Spiro-CN
2. Experimental Details
3. Determination method of  $\phi_{\text{prompt}}$  and  $\phi_{\text{delayed}}$
4. Experimental data
  - 4-1 Transient PL spectrum of Spiro-CN in toluene solution
  - 4-2 Transient PL spectrum of 6 wt% Spiro-CN: $\alpha$ -NPD co-deposited films
  - 4-3 Triplet formation efficiency of Spiro-CN
  - 4-4 Luminance-current density characteristics
5. Complete Reference 18

## 1 Synthesis of Spiro-CN

The bipolar compound comprises a cyano-substituted biphenyl branch as the acceptor orthogonally bridged to a donor branch bearing di-*p*-tolylamino group via a  $sp^3$ -hybridized carbon. Scheme 1 presents our synthetic routes toward this bipolar molecule. Starting from 2,7-dicyano-9,9'-spirobifluorene (**1**), which was reacted with  $I_2$  and  $HIO_3$  in  $AcOH$  and  $CHCl_3$  to give 2,2'-diiodo-9,9'-spirobifluorene (**2**) in 80% yield. Subsequent Pd-catalyzed C–N bond formation through the cross-coupling of the diiodospirobifluorene **2** with di(*p*-tolyl)amine afforded the bipolar **Spiro-CN** in 60% yield. The detail synthetic procedures and structural characterizations have been reported in the literature<sup>1</sup>.



Synthesis scheme of Spiro-CN

<sup>1</sup> Ku S.-Y., Hung W.-Y., Chen C.-W., Yang S.-W., Mondal E., Chi Y., Wong K.-T. *Chem. Asian J.* **2011**, DOI: 10.1002/asia.201100467.

## 2 Experimental Details

The Spiro-CN: mCP (100 nm) co-deposited films were fabricated by thermal deposition. The film thickness was monitored in-situ by an oscillating quartz thickness monitor during thermal deposition process. Fluorescence and TADF characteristics were measured under vacuum using a streak camera system (C4334, Hamamatsu Co.). Temperature dependence of PL properties were measured using a streak camera system (C4334, Hamamatsu Co.) equipped with a cryostat (GASESCRT-006-2000, IWATANI Co.) A nitrogen gas laser (MNL200, LASERTECHNIK BERLIN) with an excitation wavelength of 337nm was used. Excitation light was absolutely cut off by putting a 370 nm long band-pass filter (SCF-50S-37L, SIGMA KOKI CO., LTD.) in front of the photo-detector. PL quantum efficiency was measured using integrating sphere system (C9920-02, HAMAMATSU Co.) with a multichannel spectrometer (PMA-11, HAMAMATSU Co.) The current density-voltage-luminance (J-V-L) characteristics were measured using a semiconductor parameter analyzer (Agilent Co., HP4155C) with an optical power meter (Newport, Model 1835-C). AFM measurement was conducted by using JSPM-5400, JEOL.

## 3 Determination method of $\phi_{\text{prompt}}$ and $\phi_{\text{delayed}}$

In this study,  $\phi_{\text{prompt}}$  and  $\phi_{\text{delayed}}$  were determined by using total PL quantum efficiency and the ratio between prompt and delayed components which was calculated from transient PL measurements. The intensity ratio between prompt ( $r_1$ ) and delayed ( $r_2$ ) components were determined using emission life time ( $\tau_1$ ,  $\tau_2$ ) and fitting parameter ( $A_1$ ,  $A_2$ ) as follow.

$$I(t) = A_1 e^{-\frac{t}{\tau_1}} + A_2 e^{-\frac{t}{\tau_2}} \quad (1)$$

$$r_1 = \frac{A_1 \tau_1}{A_1 \tau_1 + A_2 \tau_2} \quad (2)$$

$$r_2 = \frac{A_2 \tau_2}{A_1 \tau_1 + A_2 \tau_2} \quad (3)$$

Then,  $\phi_{\text{prompt}}$  and  $\phi_{\text{delayed}}$  were determined using intensity ratio ( $r_1$ ,  $r_2$ ) and total emission quantum yield.

$$\Phi_{\text{total}} = \Phi_{\text{prompt}} + \Phi_{\text{delayed}} \quad (4)$$

$$\Phi_{\text{prompt}} = r_1 \Phi_{\text{total}} \quad (5)$$

$$\Phi_{\text{delayed}} = r_2 \Phi_{\text{total}} \quad (6)$$

## 4 Experimental Data

### 4-1 Transient PL spectrum of Spiro-CN in toluene solution

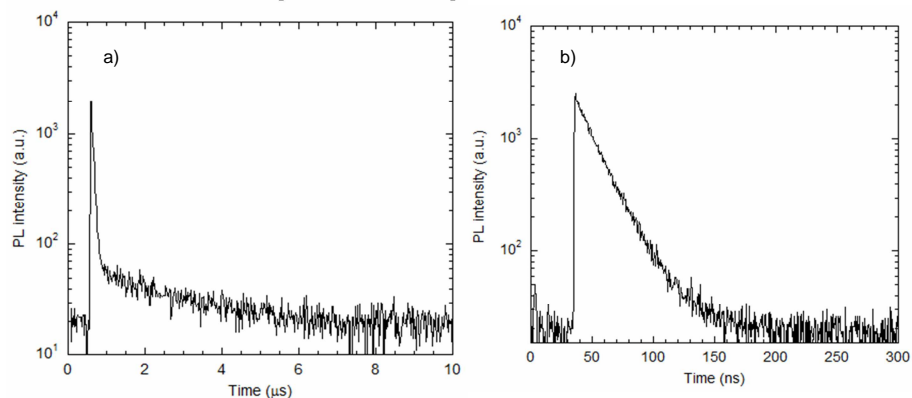


**Fig. S1.** Transient PL spectrum of Spiro-CN toluene solution ( $1.3 \times 10^{-5}$  M). (a) with nitrogen bubbling (without containing oxygen). (b) without nitrogen bubbling (containing oxygen).

### 4-2 Transient PL spectrum of 6 wt% Spiro-CN:NPD co-deposited films

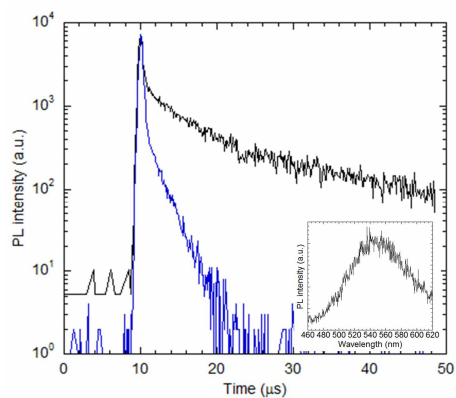


**Fig. S2.** Transient PL spectrum of 6wt % spiro-CN:  $\alpha$ -NPD co-deposited film (blue line) and 6wt% Spiro-CN: mCP co-deposited film (black line). Inset: PL spectrum of 6wt % spiro-CN:  $\alpha$ -NPD co-deposited film.

### 4-3 Triplet formation efficiency of Spiro-CN

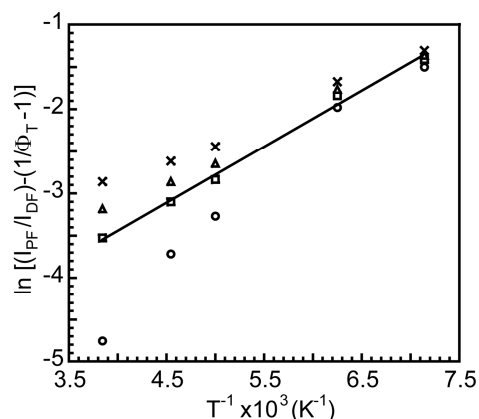


**Fig. S3.** Fit of  $I_{PF}/I_{DF}$  vs  $1/T$ .  $\Phi_T = 0.80$  ( $\times$ ),  $0.79$  ( $\Delta$ ),  $0.78$  ( $\square$ ) and  $0.77$  ( $\circ$ ). The best linear fitting was obtained when  $\Phi_T$  is  $0.78$ .

For the Berberan-Santos plot, the shape of the slope is very sensitive to the function of  $\phi_T$ . Continuous variation of this parameter in the search for the maximum linearity gives the best value of  $\phi_T$  as well as  $\Delta E_{ST}$ .<sup>2</sup> As shown in Fig. S6, the best linear fitting was obtained when  $\phi_T$  is  $0.78$ . Based on this method, the triplet formation efficiency of Spiro-CN was obtained to be  $\phi_T = 0.78$ .

<sup>2</sup> Berberan-Santos, M. N.; Garcia, J. M. M. *J. Am. Chem. Soc.* **1996**, *118*, 9391.

### 4-4 Luminance-current density characteristics

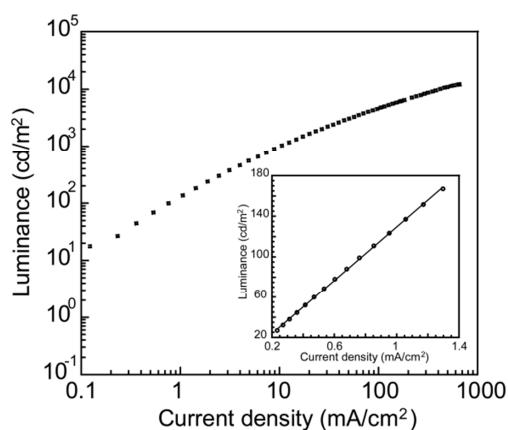


**Fig. S4.** Luminance-current density characteristics for glass/ITO/ $\alpha$ -NPD (60 nm)/6wt% Spiro-CN:mCP (20 nm)/Bphen (40 nm)/MgAg (100 nm)/Ag (20 nm). Inset shows luminance-current density characteristics at low current density region.

## 5 Complete Reference 18

(18) Gaussian 09, Revision A.02, Frisch, M. J.; Trucks, G. W. ; Schlegel, H. B. ; Scuseria, G. E.; Robb, M. A.; Cheeseman, J. R.; Scalmani, G. ; Barone, V. ; Mennucci, B.; Petersson, G. A. ; Nakatsuji, H. ; Caricato, M.; Li, X.; Hratchian, H. P.; Izmaylov, A. F.; Bloino, J. ; Zheng, G.; Sonnenberg, J. L.; Hada, M.; Ehara, M. ; Toyota, K.; Fukuda, R.; Hasegawa, J.; Ishida, M.; Nakajima, T.; Honda, Y.; Kitao, O.; Nakai, H.; Vreven, T.; Montgomery, Jr., J. A.; Peralta, J. E.; Ogliaro, F.; Bearpark, M.; Heyd, J. J.; Brothers, E.; Kudin, K. N.; Staroverov, V. N.; Kobayashi, R.; Normand, J.; Raghavachari, K.; Rendell, A.; Burant, J. C.; Iyengar, S. S.; Tomasi, J.; Cossi, M.; Rega, N.; Millam, J. M.; Klene, M.; Knox, J. E.; Cross, J. B.; Bakken, V.; Adamo, C. ; Jaramillo, J.; Gomperts, R.; Stratmann, R. E.; Yazyev, O.; Austin, A. J.; Cammi, R.; Pomelli, C.; Ochterski, J. W.; Martin, R. L.; Morokuma, K.; Zakrzewski, V. G.; Voth, G. A.; Salvador, P.; Dannenberg, J. J.; Dapprich, S.; Daniels, A. D.; Farkas, O.; Foresman, J. B.; Ortiz, J. V.; Cioslowski, J.; Fox, D. J. Gaussian, Inc., Wallingford CT, 2009.